European Polymer Journal 195 (2023) 112239

Contents lists available at ScienceDirect

European Polymer Journal

journal homepage: www.elsevier.com/locate/europolj

Mechanically-reinforced biocompatible hydrogels based on poly (N-isopropylacrylamide) and star-shaped polycaprolactones

Giacomo Damonte [a], Martina Cozzani [a], Donatella Di Lisa [b], Laura Pastorino [b], Alberto Mariani [c], Orietta Monticelli [a,*]

[a] Dipartimento di Chimica e Chimica Industriale, Università di Genova, Via Dodecaneso 31, 16146 Genova, Italy
[b] Dipartimento di Informatica, Bioingegneria, Robotica e Ingegneria dei Sistemi, Università di Genova, Via All'Opera Pia 13, 16145 Genova, Italy
[c] Dipartimento di Chimica e Farmacia, Università di Sassari, and INSTM, Via Vienna 2, 07100 Sassari, Italy

ARTICLE INFO

Keywords:
poly(N-isopropylacrylamide)
Polycaprolactone
Star-shaped polymers
Hydrogels
Frontal polymerization
Drug delivery

ABSTRACT

The aim of this work was to improve the properties of hydrogels based on poly(N-isopropyl acrylamide) (PNIPAAm) in terms of mechanical features and functionality by combining the polymer with a star-shaped tetrafunctional polycaprolactone (PCL), which was synthesized *ad-hoc* and introduced into the reaction mixture. The synthesized PCL (coded as PCL-COOH), selected to maintain the biocompatibility of the final material, was designed with a star structure characterized by four strong arms ending with maleic groups to increase the functionalization potential capable of participating in the radical polymerization and adding acid groups to the system. Specifically, various hydrogels were prepared by partially replacing pentaerytritol tetraacrylate (PE-TA), a commercial crosslinker, with increasing concentrations of PCL-COOH in the presence of trihexyl(tetradecyl) phosphonium persulfate (TETDPPS) as non-gas-releasing radical initiator. In addition, frontal polymerization (FP) was employed, a fast and energy efficient technique, potentially capable of promoting the dispersibility of PCL in the polymer matrix.

The influence of the star-shaped PCL on the polymerization process as well as on the hydrogel properties in terms of chemical structure, swelling behaviour, thermal and mechanical features was investigated. Indeed, it was found that the presence of PCL allowed the formation of a stable polymerization front up to a concentration of 25 wt%. FT-IR measurements allowed to evaluate the fraction of PCL effectively bonded to the hydrogel structure, while the morphological analysis performed by FE-SEM characterization revealed that the hydrogel pore size tended to decrease as the amount of PCL in the system increased. In addition, the star-shaped PCL was found to affect the material swelling properties, by reducing the swelling ratio without affecting the thermoresponsive behavior. Mechanical tests performed on the neat PNIPAAm hydrogels and on PCL-containing hydrogels, showed a relevant increase in the material stiffness due to the PCL-COOH addition. The DSC characterization results showed a decrease in the glass transition temperature with increasing PCL-COOH content, indicating a partial miscibility of the two polymers likely due to a compatibilization effect of a copolymer formed during the polymerization process. To demonstrate the capability of the hydrogels to retain positively charged molecules, the prepared systems were contacted with solutions containing pararosaniline hydrochloride. The retention capacity as well as the kinetic release were investigated. The measurements evidenced a higher retaining capacity and a lower release rate in the PCL-containing hydrogels. Finally, the biocompatibility and the low citoxicity of the PNIPAAm/PCL hydrogels were confirmed by a cell viability assay using the SH-SY5Y cell line.

1. Introduction

Poly(N-isopropylacrylamide) represents one of the most promising polymers applied for the preparation of hydrogels. Indeed, PNIPAAm is a thermoresponsive biocompatible polymer used for the development of smart materials with potential biomedical applications, such as controlled scaffolds for tissue engineering, wound dressings, and drug delivery systems [1,2]. However, despite the appealing properties of

* Corresponding author.
E-mail address: orietta.monticelli@unige.it (O. Monticelli).

https://doi.org/10.1016/j.eurpolymj.2023.112239
Received 12 May 2023; Received in revised form 7 June 2023; Accepted 17 June 2023
Available online 19 June 2023

PNIPAAm-based hydrogels, they have drawbacks, particularly in terms of mechanical and retention properties. Regarding the latter, the chemical structure of PNIPAAm is devoid of functional chain groups, which limits both ionic and covalent interactions required for binding with target molecules. In particular, the lack of functionality was found to make the incorporation of hydrophobic drugs very difficult especially below the lower critical solution temperature (LCST) [3]. At the same time, PNIPAAm-based hydrogels lack mechanical strength, due to high water uptake and the resulting low density of polymer chains in the swollen hydrogel, limits their use for structural applications [4,5]. To address the above drawback, various approaches were explored by adding one or more components to NIPAAm in the form of monomers, polymers, or fillers [4]. Indeed, it is worth underlining that a direct comparison among the values of the mechanical parameters of the different studied systems is difficult because the mechanical behaviour is influenced by several variables, such as the degree of swelling, the applied temperature, the measuring method, etc. Nevertheless, among the various proposed approaches, some resulted to be the most effective. In particular, PNIPAAm-based interpenetrated networks (IPN) hydrogels, developed mainly to modify swelling behaviour, showed improvement in mechanical properties [4]. For example, Petrusic et al. prepared thermoresponsive IPN hydrogels that achieved a modulus of 120 KPa by reinforcing a PNIPAAm network with calcium alginate [6]. It was found that another approach to improve the mechanical properties of PNIPAAm-based hydrogels is based on double networks (DN), *i.e.*, a type of IPN in which the degree of crosslinking between the two polymeric networks is asymmetric [7–9]. In this case, in order to improve the mechanical properties, the first network should be able to swell sufficiently in the second and consequently be less crosslinked. Using this strategy, Fei et al. prepared P(NIPAAm-*co*-2-acrylamido-2-methylpropane sulfonic acid)/PNIPAAm DN hydrogels that achieved a compressive modulus of 340 KPa [8].

In addition, the incorporation of fillers/nanofillers, such as graphene oxide (GO) [9,10], silica [11,12], Fe_2O_3 [13], Au nanoparticles [14], TiO_2 [15] and clay [16,17] was found to play a role in the improvement of the mechanical behaviour of hydrogels. In this case, the compatibility of the fillers and the non-simple dispersion have to be considered [18]. These works, demonstrating the interest in developing methods to modify the properties of PNIPAAm-based hydrogels, generally focused on improving a single property. The development of an approach to overcome the various drawbacks associated with these materials is therefore of great interest.

In the field of coupling polymers with monomers and polymers - a method essentially used to functionalize the matrix and modify its LCST - few works focused on polycaprolactone (PCL), namely the polymer objective of the work. Indeed, as far as we know in all the works published so far, PCL was combined with PNIPAAm in the form of a copolymer. In particular, in NIPAAM/PCL-based block copolymer hydrogels, various forms of PCL have been used as crosslinkers. However, they all had a linear structure. Indeed, it was introduced in the form of PCL-diacrylate [19], PCL-methacrylate [20] or PCL-hydroxyethylmethacrylate macromonomer [21] with the main purpose of introducing a hydrolysable degradable fraction in PNIPAAm, rather than improving its mechanical properties.

In our work, a new formulation was developed by polymerizing NIPAAm with an *ad-hoc* developed polymer potentially capable of improving some of the properties of the matrix without changing its biocompatibility. A star-shaped tetrafunctional PCL, characterized by maleic end groups (PCL-COOH) and thus capable of participating in radical polymerization and conferring acid functionalities to the system, was synthesized and added to the polymerization mixture at different concentrations (Fig. 1). The decision to use a star-shaped polymer, which is a novelty in the current literature, is related to the fact that the synthesized polymer contains a greater number of functionals groups compared to a linear system with the same molecular weight. This property can significantly affect the ability of the macromolecule to be covalently inserted into the hydrogel system, thanks to the reactivity of the double bond, and promoting the network crosslinking, thanks to the tetrafunctional structure. In addition, the high number of the carboxyl end groups of the star-shaped polymer, always compared to a linear structure, can significantly increase the material ability to interact with positively charged molecules.

Moreover, frontal polymerization, a fast and energy-efficient method, was applied to promote PCL dispersion in PNIPAAm matrix, by "freezing" the homogeneity of the polymerization mixture [22].

Frontal polymerization can indeed be considered an "energy-efficient" approach, since the only external energy required for frontal polymerization is an initial thermal stimulus that ignites the reaction locally. It is the exothermicity of the reaction that provides local heating, and the transfer of this thermal energy to adjacent monomers in the reaction medium results in a self-sustaining reaction zone that produces fully cured thermosets and thermoplastics. The propagation of this

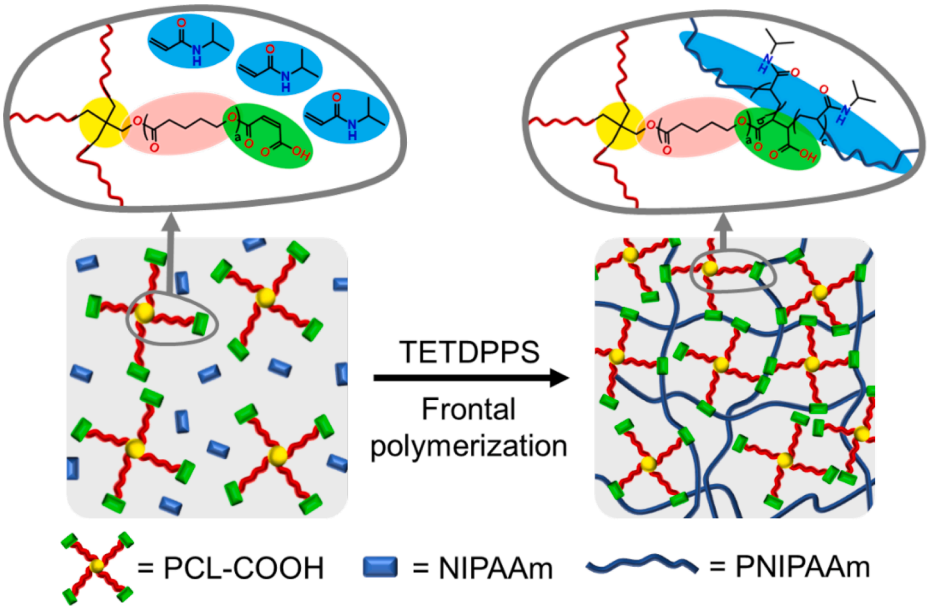

Fig. 1. Scheme of the developed PNIPAAm/PCL hydrogels.

polymerization front continues through the unreacted monomer medium until either all reactants are consumed or sufficient heat loss stops further reaction [22].

The prepared hydrogels were fully characterized by IR, DSC, TGA, FE-SEM, swelling and mechanical measurements. Dye retention and release tests were performed to assess the binding capacity of hydrogels towards PR (pararosaniline hydrochloride), a triarylmethane cationic dye. Cell viability tests were performed using SH-SY5Y cell line to prove the biocompatibility of the material.

2. Materials and methods

2.1. Materials

N-isopropylacrylamide (NIPAAm, purity ≥ 97%), ε-caprolactone (ε-CL, purity = 97%), dimetylsulfoxide (DMSO, purity ≥ 99%), aliquat 336 chloride (AQC, purity ≥ 98%), ammonium persulphate (APS, purity ≥ 98 %), pentaerythritol (purity = 99%), pentaerythritol tetraacrylate (PE-TA, with 350 ppm hydroquinone monomethyl ether), tin octoate (Sn(Oct)$_2$, purity ≥ 96%), methanol (99.9%), maleic anhydride (purity ≥ 99%), diethyl ether (purity 99 %, stabilized with BHT), toluene (purity = 99.8%, anhydrous), pararosaniline hydrochloride (PR, purity ≥ 85 %), N-methyl pyrrolidone (NMP, purity ≥ 99.5 %, anhydrous), 2,2′-azobis(2-methylpropionitrile) (AIBN, purity ≥ 98.0 %), benzoyl peroxide (BPO, with 25 % water, for synthesis) and dichloromethane (DCM, purity ≥ 99.8%, stabilized with amylene) were purchased from Sigma Aldrich®. Trihexyl tetradecyl phosphonium chloride (TETDPC, purity ≥ 97%) was purchased from TCI chemicals. ε-caprolactone and DCM were purified prior to use by vacuum distillation over CaH_2 and stored under Ar atmosphere. Diethyl ether was purified by distillation to remove inhibitor prior to use. Pentaerythritol was dried in vacuum oven at 40 °C prior use. BPO was dried before use. All the other reagents were of analytical grade and used without further purification.

2.2. Synthesis of maleated star-shaped PCL (PCL-COOH) and initiators

The tetrafunctional maleated star PCL (PCL-COOH) was prepared by esterification of an hydroxyl-terminated star tetrafunctional PCL (PCL-OH) with molecular weight ($M_{n,NMR}$) of 2000 g/mol per arm, following a procedure already reported in the literature [23–26]. FT-IR and ^{1}H NMR signals for PCL-OH and PCL-COOH, are reported in the Table S1 of the Supporting Information. Aliquat persulphate (AQPS) was prepared according to a previous procedure reported by Masere et al. by metathesis reaction between APS and AQC [27], whereas for the synthesis of trihexyl tetradecyl phosphonium persulphate (TETDPPS), the procedure reported by Mariani et al. by metathesis reaction between TETDPC and APS was used [28].

2.3. Preparation of poly(NIPAAm)/PCL-COOH hydrogels

The polymerization process was studied preliminarly by determining the type of solvent and the minimum concentration for the solubilization of NIPAAm and PCL-COOH. Indeed, NMP and DMSO were tested by contacting the solvents with 1 g of NIPAAm (Table S2). To determine the minimum amount of solvent required to dissolve a mixture of 1 g of NIPAAm and 0.5 g PCL-COOH, different amounts of DMSO, which was found to be the optimal solvent, were added to the above mixture. In order to carry out the frontal polymerization in the optimized conditions, 5 g of NIPAAm were dissolved in 3 mL of DMSO inside a glass test tube (13 mm internal diameter and 100 mm length), with mechanical stirring, followed by the appropriate amount of crosslinker (PETA or a mixture of PETA and PCL-COOH as reported in Table 1 for sake of convinience). After complete dissolution of the solids, 150 mg (0.5 mol% respect to NIPAAm) of TETDPPS were added and stirred for an additional 30 s. FP of the samples was then initiated by heating the outer wall of the upper part of the test tube with the tip of a tin welder (450 °C).

Table 1
Characteristics of the prepared NIPAAm-based hydrogels.

Sample code	PETA/PCL ratio[1]	PCL content[2] [m/m%]	PCL content[2] [mol%]	PETA[3] [mg]	PCL[3] [mg]
PNIP_F	100/0	0	0	100	0
PNIP_PCL_10_F	80/20	10	0.132	80	500
PNIP_PCL_20_F	60/40	20	0.264	60	1000
PNIP_PCL_25_F	50/50	25	0.33	50	1250

Crosslinker content, expressed as the sum of PETA and PCL-COOH respect NIPAAm moles, was 0.66 mol%. [1]PETA/PCL indicates the composition of the crosslinking fraction added to NIPAAm expressed as mol/mol ratio respect the total amount of crosslinker. [2]PCL content is calculated respect NIPAAm. [3]PETA and PCL are expressed as the quantity required for 5 g of NIPAAm.

After polymerization, the hydrogels were carefully removed by breaking the tube, sliced in the desired shape, and immersed in milliQ water for 5 days, changing the water every day to remove DMSO and other water-soluble contaminants.

2.4. Characterization

^{1}H NMR proton spectroscopy was performed with a Jeol ECZ400R/S3 400 MHz by using 10 mm NMR test tubes and $CDCl_3$ as solvent. The samples, priorly dissolved in $CDCl_3$ at a concentration of 30 mg/mL, were analyzed at room temperature.

FT-IR spectra of the xerogels were recorded in ATR from 400 to 4000 cm^{-1} using a Bruker "Vertex 70®". To estimate the quantity of covalently bound PCL in the structure, the samples were subjected to an extraction process performed by soaking the materials for 24 h in an excess of DCM, a good solvent for PCL. After extraction, the samples were dried in a vacuum oven for several days at room temperature and analysed. The PCL content was then determined by plotting the areas for the C═O stretching peak of PCL at 1725 cm^{-1} vs. the PCL content of dried, unwashed xerogels to obtain a calibration curve for PCL. The concentration of PCL-COOH in the extracted samples was then calculated by measuring the area in the same way and inserting it into the calibration curve.

Thermal analysis of the samples was performed on xerogels with a Mettler Toledo differential scanning calorimeter (DSC1 STAR^e System®), between −100 and 150 °C, at a heating/cooling rate of ± 10 °C/min and an N_2 flow of 20 mL/min. The crystallinity degree (X_c) of PCL in the xerogels was calculated based on their PCL contents, Φ_{PCL}, following the Eq. (1). Thermogravimetric analysis (TGA) was performed in the range 30–800 °C under inert atmosphere with an N_2 flow of 80 mL/min.

$$X_c(\%) = \frac{\Delta H_m}{\Delta H_m^0 \times \varphi_{PCL}} \times 100\% \quad (1)$$

where ΔH_m = measured melting enthalpy, Φ_{PCL} = PCL weight fraction in the xerogel and ΔH_m^0 is the melting enthalpy of a 100% crystalline PCL, considered as 139 J/g [29].

For the above calculation, the second heating scan was considered. The temperature of the front during FP was measured using a K-type thermocouple inserted into the reaction mixture at 2 cm from the bottom of the test tube. The temperature change was then monitored by a digital thermometer. The polymerized samples were obtained by carefully breaking the test tube, cut into pieces, and washed in milliQ water for 5 days, changing water every 24 h. After washing, the samples were dried in a vacuum oven at room temperature, until constant weight. Swelling ratio was measured from 20 to 70 °C on small hydrogel disks (5 mm diameter, 3 mm of thickness) using milliQ water as solvent and increasing the water bath temperature by 5 °C/day (2 °C/day between 30 and 40 °C for improved LCST resolution). The swelling ratio % (SR%) was then obtained by applying Eq. (2).

$$SR\% = \frac{M_s - M_i}{M_i} \cdot 100 \quad (2)$$

Where M_s and M_i are the weight of the swollen hydrogel and dried xerogel respectively.

Field emission scanning electron microscopy (FE-SEM) was performed with a Zeiss Supra 40 VP equipped with a backscattered electron detector. The freeze-dried samples were immersed in liquid nitrogen, cryogenically fractured and thinly sputter-coated with carbon using a Polaron E5100 sputter coater prior to analysis. Statistical analysis of pore size in xerogels was performed by using ImageJ software.

Mechanical tests were performed using a Zwick/Roell Z0.5 electromechanical testing machine (Standards EN 2562–EN 2746) equipped with a planar support. For this characterization, swollen samples were prepared punching out into a small round slice with a hole puncher (Ø = 5 mm in diameter and h = 2 mm); the tests were run at a rate of 1 mm/min. The modulus of hydrogels was obtained by compressing the samples at a strain rate of 20–25%. Moreover, indentation tests were performed using a prototype DMA apparatus, consisting of a mini-shaker operating in a range between 1 Hz and 10 KHz with maximum force of 1.5 N, a laser vibrometer to measure the displacement, set at 80 μm/V and a force transducer. All tests were run on swollen cylindrical samples (Ø = 5 mm in diameter and h = 1 mm) at 22 °C. The samples were place on a plate connected with the shaker, a cylindrical indenter of 5 mm in diameter was approached until touching the upper surface of the sample and then 20% pre-strain has been applied. The test was run with an oscillation between 2 Hz and 100 Hz and the sinusoidal signal of the displacement and of the force, respectively response and stimulus, was elaborated by the software producing a spectrum containing the storage modulus and the loss modulus vs. the frequency. Both mechanical tests were performed at room temperature.

2.5. Dye absorption and release tests

Xerogel disks prepared by cutting hydrogel pieces 5 mm in diameter and 2 mm thick were individually immersed in 5 mL of pararosaniline dye solution (5 μg/mL) for 24 h, in the dark at 22 °C. After this time, the concentration in the surnatant was analyzed by means of UV–Vis spectrometry. The corrected concentration was determined by considering the amount of water retained by the dried hydrogels during the absorption time, based on their weight change from the dry to the swollen state in swelling test, and then applying the following Eqs. (3) and (4):

$$C_{CORR} = \frac{C_1 V_1}{V_2} \tag{3}$$

$$\text{Dye absorbed} = \frac{(C_i - C_{CORR}) \cdot V_2}{m_{dry}} \tag{4}$$

Where C_1 is the measured concentration, V_1 is 5 mL – X mL of water absorbed by the xerogel during the swelling phase, C_{CORR} is the corrected concentration and V_2 = 5 mL. C_i = initial concentration, m_{dry} = initial mass of the dried xerogel disk.

All the concentrations were expressed in μg/mL. The quantity of dye absorbed by the materials was expressed as μg/g of dried xerogel. The dye release tests were performed in the same manner as the dye adsorption tests, but a more concentrated solutions (100 μg/mL) was used. The hydrogel disks were then removed, externally dried by gently tapping with a paper towel, and immersed in 5 mL of milliQ water at 22 °C. Dye release was followed by means of UV–Vis spectrometry until a plateau was reached in the measured absorbance.

2.6. Cell culture conditions and viability evaluation

The human neuroblastoma cell line SH-SY5Y was grown in 75 cm^2 tissue culture flasks in complete Dulbecco's modified Eagle's medium (DMEM (4.5 g/L)) supplemented with 10% fetal bovine serum (FBS), 1% penicillin–streptomycin and 1% glutamax, at 37 °C in 5% CO_2. The day before plating, the samples were sterilized in 70% ethanol for 40 min, then washed three times in H_2O and normalized overnight in culture medium. For all experiments, cells were plated in 6-well plates at a density of $2{\cdot}10^5$ cells/well in 2 mL of culture medium. After 24 h, the samples were placed in 40 μm cell strainers and then in 6-well plates for 48 h, to evaluate the cytotoxic effect of substances leaching from the samples. Cells were observed before and after the exposition to the samples and every 24 h, acquiring contrast phase images by an inverted IX-51 Olympus microscope equipped with a DP70 digital camera. The survival rate of cells was observed after 48 h of culture. Cell viability was assessed using a standard live/dead™ assay (calcein AM/ethidium homodimer) according to the manufacturer's instructions. To perform the assay, 1 mL of the staining solution containing 0.50 μL of calcein AM and 2 μL of ethidium homodimer in DPBS was used to replace the cell culture medium, followed by incubation in the dark at 37 °C for 20 min. Live and dead cells were imaged using Olympus BX-51 upright microscope equipped with a Hamamatsu Orca ER II digital cooled CCD camera driven by Image ProPlus software (Media Cybernetic) at excitation/emission wavelengths of 494/515 nm for calcein (green, live cells) and 528/617 nm for ethidium homodimer-1 (red, dead cells). NIH ImageJ software was used to quantify the cell viability based on the ratio of the live cell number to the total number of cells.

3. Results and discussion

3.1. Optimization of the polymerization conditions

This work preliminarily focused on the optimization of the polymerization process, including the type of solvent and initiator as well as the monomer concentration. Regarding the solvent, some properties were considered, namely the water solubility and the ability to dissolve both the system components, namely NIPAAm and the star-shaped PCL. Indeed, it is worth underling that in order to perform the FP process, the solutions should be sufficiently concentrated to generate an appropriate thermal output and allowing for the propagation front to self-sustain. The behavior of NMP and DMSO was evaluated by carrying out a preliminary solubility test with NIPAAm. From the results shown in Table S2, it results that the use of DMSO allowed the preparation of NIPAAM solutions characterized by a higher concentration than those prepared using NMP. Based on the above results, DMSO was chosen, and the minimum amount of solvent required to solubilize a system consisting of NIPAAm and PCL-COOH was determined. The polymerization condition assessment also considered the selection of the most suitable radical initiator. Indeed, by using some classical radical initiators such as BPO and AIBN, particularly at high concentration, the formation of bubbles and defects within the gel during FP was observed, which might affect the mechanical properties of the material as well as the maintenance of a stable polymerization front during the FP process [30]. Moreover, the compounds generally used to obtain polymers based on NIPAAm are initiators that do not release gas, such as potassium [31,32] or ammonium [33,34] persulphates, which being soluble in highly polar media, cannot be used in our system. As such in this work, we considered the exploitation of persulphates soluble in organic solvents, such as AQPS [27] or TETDPPS [28]. Among the above two compounds, TETDPPS was chosen as it allowed to obtain a stable polymerization front.

The FP process was studied by evaluating the front position as a function of time (Fig. S1). Fig. S1 shows, as an example, the position of the front as a function of time for the sample with the highest amount of PCL-COOH, namely PNIP_PCL_25_F. A very similar trend was observed for all the other synthesized systems. Indeed, the experimental data fitted by a straight line demonstrated that the polymerization proceeds at a constant velocity and thus that a pure FP occurs. Moreover, it is relevant to underline that the presence of PCL-COOH did not negatively affect the frontal polymerization process, at least at the concentrations used.

The front velocity (V_f) as well as the front temperature (T_f) for all the

prepared systems are given in Table S3. The above results indicate that the addition of the star-shaped polymer to the reaction mixture decreased both the above parameters, with V_f going from 0.47 cm·min^{-1} for PNIP_F to 0.20 cm·min^{-1} for PNIP_PCL_25_F, while T_f, which was 135 °C for the neat PNIPAAm hydrogel, was reduced to 93 °C for the sample with the highest PCL content, PNIP_PCL_25_F. This finding may be attributed to a "diluting" effect of PCL-COOH, which, although characterized by double bonds and thus capable of participating in the polymerization process, is characterized by a low content of reacting groups as compared to its total mass, thus acting as heat sink much more than what NIPAAm does. Since frontal polymerization requires a certain amount of energy to propagate, it can be hypothesized that PCL-COOH limits the front formation at a certain concentration. Indeed, it was found that at a concentration of more than 25 wt% of the star-shaped polymer with respect to the monomer, a self-sustaining reaction front could not be achieved after initiation, likely due to the limited thermal output. Therefore, the above concentration was the highest used to develop the hydrogel by frontal polymerization.

3.2. FT-IR measurements

FT-IR spectra of the PNIPAAm-based xerogels are showed in Fig. 2. In PNIP_F, the sample prepared by using neat NIPAAm as monomer, the presence of signals clearly attributable to PNIPAAm was observed at: 3410 cm^{-1} (υ O–H, water), 3283 cm^{-1} (υ N–H), 2973 cm^{-1} (υ C–H asymmetric/symmetric), 2877 cm^{-1} (υ C–H asymmetric/symmetric isopropyl group), 1626 cm^{-1} (amide I band) and 1541 cm^{-1} (amide II band). The above bands are consistent with those previously reported by other authors [35]. In contrast, the analysis of the samples containing the star-shaped polymer showed additional peaks attributed to PCL chains at: 2950 cm^{-1} and 2870 cm^{-1} (υ Csp3- H methyleneic unit), 1725 cm^{-1} (υ C = O), at 1295 cm^{-1} (υ C–O and C–C), 1242 cm^{-1} and 1171 cm^{-1} (υ C–O–C asymmetric/symmetric), which are in good agreement with the results of previous studies [36,37]. In particular, the area of the peak belonging to υ C═O of PCL, at 1725 cm^{-1}, showed a good correlation with the PCL concentration in the sample, increasing with the PCL content. At the same time, the intensity of the PNIPAAm signals decreased, which can be attributed to a decrease in the PNIPAAm content in the xerogels. This trend was also reflected in the intensity of the O–H stretching at 3410 cm^{-1} caused by the water retained by the PNIPAAm backbone. This signal, which partially overlapped with N–H stretching of PNIPAAm, was reduced by the presence of PCL. These findings suggest that the addition of a hydrophobic polyester such as PCL can alter and reduce the water uptake of the xerogels structure. It can be deduced that the incorporation of PCL in the gel structure can lead to a change in the properties of the resulting materials, including their water affinity.

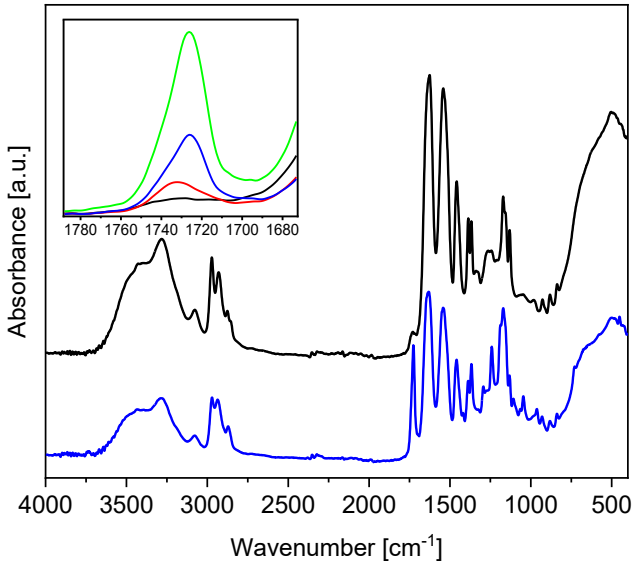

Fig. 2. FT-IR spectra of PNIP_F (black), PNIP_PCL_10_F (red), PNIP_PCL_20_F (blue), PNIP_PCL_25_F (green). (For interpretation of the references to colour in this figure legend, the reader is referred to the web version of this article.)

The conversion with respect to the monomer was calculated by weighing the gels before and after washing with water, taking into account the mass loss associated with DMSO removal (Table 2). The results reported in Table 2 indicate that a conversion of about 80% could be achieved with the frontal polymerization, a value that does not seem not to change significantly with the addition of the star-shaped polymer to the reaction mixture.

In order to estimate the fraction of PCL-COOH involved in the polymerization reaction to form star-block copolymers, the areas of the C═O peak of PCL at 1725 cm^{-1} were compared before and after the extraction of the xerogels with DCM, a good solvent for the star-shaped polymer. It is worth mentioning that the studied samples were previously washed with water. Therefore, the calculated amount of star-shaped polymer refers to PNIPAAm, i.e., to the system from which the monomer was removed. The concentration of PCL-COOH was then calculated and the percentages of bonded/unbonded PCL-COOH in the samples are reported in Table 2. This analysis provided valuable information on the efficiency of the reaction and the degree of incorporation of the polyester in the copolymer structure. Based on the results obtained, it was found that an increase in the concentration of PCL-COOH in the starting mixture led to an increase in the fraction of the polymer involved in the formation of the copolymer with NIPAAm. This increase is probably due to the fact that the probability that the maleic terminals (*i.e.*, the functional groups in PCL-COOH, which can react with NIPAAm) to participate in the radical polymerization reaction increases with increasing the concentration of PCL-COOH. This, in turn, results in a greater amount of polymer being bound to the gel matrix. Overall, this observation suggests that the concentration of PCL-COOH in the starting mixture may be a crucial factor in determining the properties of the resulting copolymer, such as its structure, composition, and mechanical properties. Further experiments may be required to further investigate the relationship between the concentration of PCL-COOH and the properties of the copolymer.

3.3. Xerogels thermal properties

The thermal behavior of xerogels was studied by DSC measurements. The DSC traces from the cooling and second heating are given in Fig. 3, while the thermal data are summarized in Table 3. For comparison, also DSC data from PCL-COOH are shown in the same table. In agreement with previous reports, neat PNIPAAm xerogels exhibited a glass transition temperature at about 140 °C [38]. It is relevant to underline that the PCL-based samples showed a relevant decrease of T_g, although it was found that the value depended on the content of the star-shaped polymer in the blend. Indeed, the T_g decreases from 140 °C in the case of PNIP_F

Table 2
PCL-COOH content after DCM extraction calculated by FT-IR measurements.

Sample	Monomer conversion[1] [%]	PCL-COOH before washing [m/m%]	PCL-COOH after washing [m/m%]	PCL-COOH bonded fraction [%]
PNIP_F	82	0	0	0
PNIP_PCL_10_F	80	10	2	20
PNIP_PCL_20_F	75	20	5	25
PNIP_PCL_25_F	78	25	7.5	30

[1] monomer conversion refers to NIPAAm and was calculated gravimetrically by weighing the gels before and after washing with water, taking into account the mass loss associated with DMSO removal.

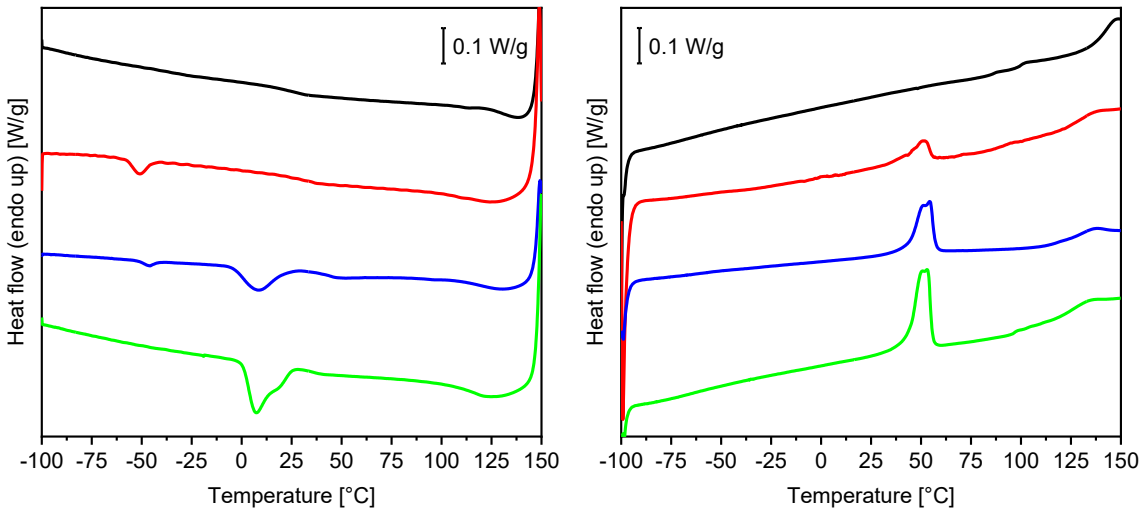

Fig. 3. DSC thermograms, cooling (left) and second heating (right), of: PNIP_F (black), PNIP_PCL_10_F (red), PNIP_PCL_20_F (blue), PNIP_PCL_25_F (green). (For interpretation of the references to colour in this figure legend, the reader is referred to the web version of this article.)

Table 3
Results from DSC analysis of PNIPAAm-based xerogels.

Sample code	T_c [°C]	$\Delta H_{c\ CORR}$ [J/g]	T_g [°C]	T_m [°C]	$\Delta H_{m\ CORR}$ [J/g]	$\chi_{c\ CORR}$ [%]
PCL-COOH	25	−71*	−60	47	70*	50*
PNIP_F	–	–	140	–	–	–
PNIP_PCL_10_F	−51	−20	135	44	51	31
PNIP_PCL_20_F	−45/8	−30	121	46	54	33
PNIP_PCL_25_F	7	−45	115	52	53	38

The subscript m and c indicate the values measured during melting and crystallization, respectively. χ_c is the degree of crystallinity calculated by assuming the ideal enthalpies of fusion as 139 J/g and considering the PCL content in the xerogel. *: the values reported for PCL-COOH were not subjected to corrections.

to 115 °C for PNIP_PCL_25_F, indicating a partial miscibility between the two polymer phases. To explain this phenomenon, as previously shown, it is necessary to consider the formation of a copolymer during the polymerization process, which can settle at the interface between the two polymer phases and increase their compatibility. Moreover, considering the PCL crystallization behavior, it is interesting to note that the crystallinity (χ_c) of PCL tended to decrease in the blend compared to the neat polymer. A slight difference was observed when the star-shaped polymer content was increased, χ_c ranging from 31% in the case of PNIP_PCL_10_F to 38% for the xerogel with the highest PCL content, PNIP_PCL_25_F. Again, these results can be explained considering that part of the PCL added to the reaction mixture is covalently bound and has a lower chain mobility, so that it can participate in the crystallization process only to a limited extent, while another part, which is mixed, can structuring. Looking at the cooling traces, we can see a very different behavior of the samples depending on the PCL content. In particular, for PNIP_PCL_10_F, a single crystallization peak was observed at a T_c of −51 °C, which was much lower than that of the neat PCL-COOH (T_c of about 25 °C). In the case of PNIP_PCL_20_F, two peaks are observed at 45 °C and 8 °C, while PNIP_PCL_25_is characterized by only one peak at 7 °C. As previously reported for other blended xerogel, e.g. based on PCL end-capped with acrylic units and poly(2-hydroxyethyl acrylate) (PHEA), the above results can be attributed to a fractioned crystallization of the PCL phase [39]. This phenomenon, which generally occurs when a semicrystalline polymer is subdivided into small domains containing less or less active heterogeneities so that nucleation and crystallization of the polymer can occur only at larger undercoolings, can be associated with the finely distributed domains of PCL in the xerogel. Indeed, the crystallization of the above domains, which could be free of nucleating impurities, may be controlled by homogeneous nucleation occurring at the maximum possible undercooling, i.e., near the glass transition temperature [40]. Of course, the phenomenon described above depends not only on the PCL content, but also on the size of the domains, which explains the different behavior of the samples. It is worth underling that PCL crystallizes at low temperatures when segregated in nanosized spheres in block copolymers [41–43] or in the interlamellar poly(lactide) regions of partially miscible poly(lactide)-block-poly(caprolactone) copolymers [44].

The thermal stability of xerogels was tested by TGA/DTG measurements, and the results are given in Fig. 4 and Table 4. An initial weight loss, $T_{onset5\%}$, below 200 °C was observed for all the samples tested, which was associated with the water molecules bound to the PNIPAAM structure by hydrogen bonds [45]. As expected, the amount of water loss in this step, which was also observed in other PNIPAAm-based systems [46–48], namely Δ_{m1}, was inversely correlated with the PCL content, and followed the trend PNIP_F > PNIP_PCL_10_F > PNIP_PCL_20_F > PNIP_PCL_25_F. Indeed, the presence of PCL, a hydrophobic and semicrystalline polymer, led to a decrease in the amount of water bound to the xerogel structure. At higher temperatures, all the samples showed similar TGA curves with a single degradation step mainly due to the statistical C–C backbone break of PNIPAAm. In the neat PNIPAAm xerogel, PNIP_F, the T_{max} measured for this step was 435 °C, in good agreement with the temperature of 420 °C reported by Schild et al. for a linear high molecular weight PNIPAAm sample [49]. For the PCL-containing samples, only a minor effect of PCL on the reduction of T_{max} was detected, which was accounted to a partial overlap between the statistical β-scission degradation step of PCL, which normally occurs at ca. 425 °C [50], and PNIPAAm degradation. Overall, these results suggest that the presence of PCL does not affect the thermal stability of the xerogels.

3.4. Swelling and thermoresponsive properties of hydrogels

Fig. 5 shows the swelling ratio % (SR%) of PNIPAAm-based hydrogels as a function of temperature. At 20 °C, the SR% of neat PNIPAAm hydrogels was in agreement with the values reported in the literature [51,52]. Indeed, the presence of PCL in the system led to a significant decrease in the swelling ratio, which ranged from about 1000% in the case of PNIP_F to 320% for the sample characterized by the highest PCL content, i.e., PNIP_PCL_25_F. As previously reported, the above phenomenon can be attributed to the intrinsic hydrophobicity of the polyester as well as to its semicrystalline structure, which is partially preserved in the blend hydrogels and appears to limit the ability of the

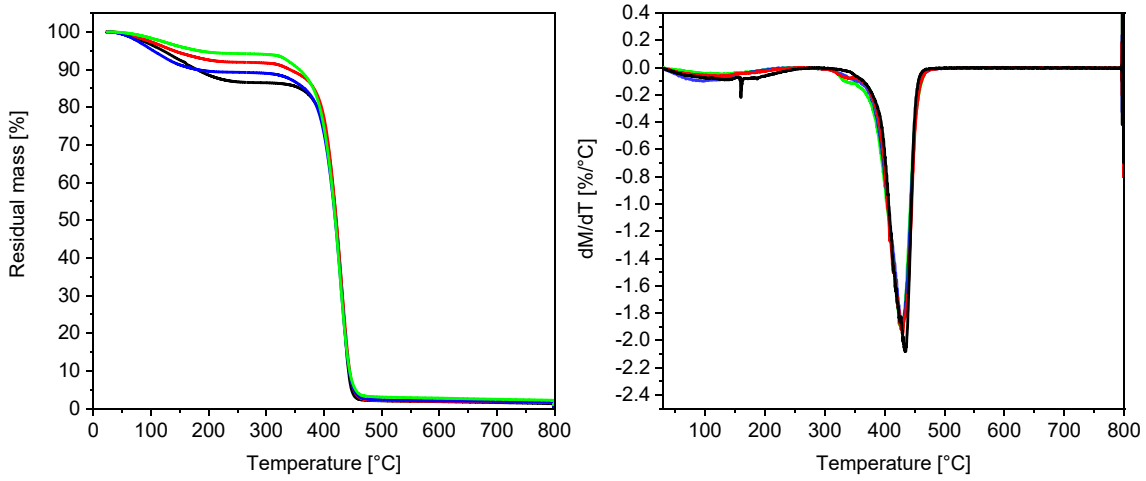

Fig. 4. TGA (left) and DTG curves (right) of: PNIP_F (black), PNIP_PCL_10_F (red), PNIP_PCL_20_F (blue), PNIP_PCL_25_F (green). (For interpretation of the references to colour in this figure legend, the reader is referred to the web version of this article.)

Table 4
Results from TGA analysis of PNIPAAm-based xerogels.

Sample code	$T_{onset5\%}$ [°C]	T_{max1}* [°C]	Δ_{m1} [%]	T_{max2}* [°C]
PCL-COOH	253	387	10	428
PNIP	80	160	13.5	435
PNIP_PCL_10_F	88	121	11.0	430
PNIP_PCL_20_F	71	106	8.2	431
PNIP_PCL_25_F	107	128	6.0	426

*:T_{max1} and T_{max2} values are extrapolated from DTG curves.

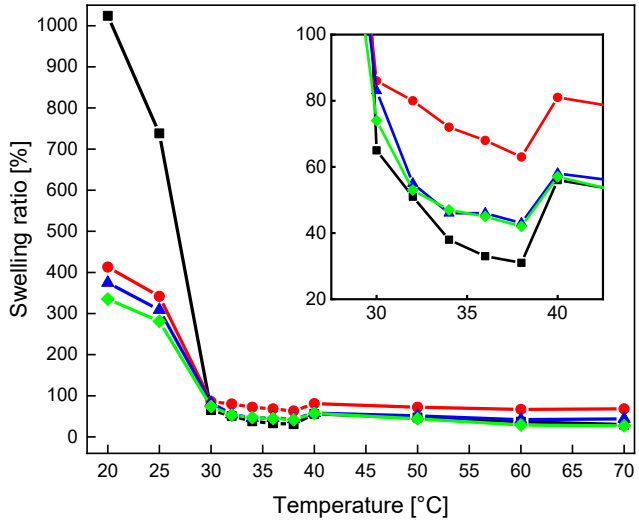

Fig. 5. Equilibrium SR% in function of temperature for PNIP_F (black), PNIP_PCL_10_F (red), PNIP_PCL_20_F (blue), PNIP_PCL_25_F (green). (For interpretation of the references to colour in this figure legend, the reader is referred to the web version of this article.)

system to retain water. Nevertheless, the values of the swelling ratio of the hydrogels containing PCL are significantly high to be used in areas where it is necessary to modify the material dimension by changing the environment [53]. In addition, it is worth underling that SR% tended to decrease when the amount of PCL in the hydrogel increased, but this variation was limited since the swelling ratio of PCL-based hydrogels ranged between 350 and 400 %. Considering the SR% of the neat PNIPAAm as a function of temperature, it showed a significant reduction with increasing temperature, demonstrating its well-established thermoresponsive behavior with a lower critical solution temperature (LCST) of ca. 32 °C [4,54]. Indeed, it was reported that when the temperature is increased, the hydrogen bonding, involving the hydrophilic amide group, is weakened and consequently, the interactions among the hydrophobic groups (–$CH(CH_3)_2$) become strong [4]. This phenomenon leads to the release of water from the structure and at the same time to the collapse of polymer chains. Considering the SR% of PCL-based samples as a function of temperature, a similar trend as the neat hydrogel was found, with a LCST, namely the temperature where the swelling ratio is the lowest and is the same for the samples, of ca. 32 °C. This result shows that the presence of the star-shaped polymer in the system affects its ability to retain water, but it is not responsible for the change in chain structure and interactions with the environment, i.e., it does not lead to a change in LCST. It is known that the modification of LCST in PNIPAAm-based hydrogels can be achieved only by forming proper random copolymers, such as those prepared e.g., from acrylic acid [55] or HEMA [56]. In our case, as previously reported, PCL forms a certain amount of copolymer, reacting with the monomer, responsible for the compatibilization of the mixed phases, but remains mainly dispersed in the PNIPAAm phase. Nevertheless, it is worth underling that the main aim of our work was indeed not to change the chemical structure of PNIPAAm, but to find a strategy to improve its features, such as mechanical properties and its ability to interact with certain types of chemicals.

3.5. Morphological analysis

The morphology of the neat PNIPAAm xerogel was compared with that of the systems containing the star-shaped PCL. Fig. 6 shows the FE-SEM micrographs of the cross-section of the synthesized freeze-dried samples, namely PNIP_F (Fig. 6a), PNIP_PCL_10_F (Fig. 6b), PNIP_PCL_20_F (Fig. 6c) and PNIP_PCL_25_F (Fig. 6d).

Although all the above samples showed a typical hydrogel sponge structure [57,58], some differences can be noted. Indeed, the size of pore diameter tended to decrease with increasing PCL content in the system. Indeed, in the case of PNIP_F, the mean pore size was of 4.02 ± 1.28 μm and decreased after PCL inclusion to 2.56 ± 0.77 μm in PNIP_PCL_10_F, 2.303 ± 0.67 μm in PNIP_PCL_20_F and 1.348 ± 0.408 μm in PNIP_PCL_25_F. From FE-SEM observations, it can be concluded that, in addition to the aforementioned properties of the hydrogels related to the hydrophobicity and crystallinity of PCL, the morphology of the PCL-based hydrogels must also be taken into account to explain their different swelling behavior compared to that of the neat PNIPAAm sample. Similar results were reported for other PNIPAAm-based systems,

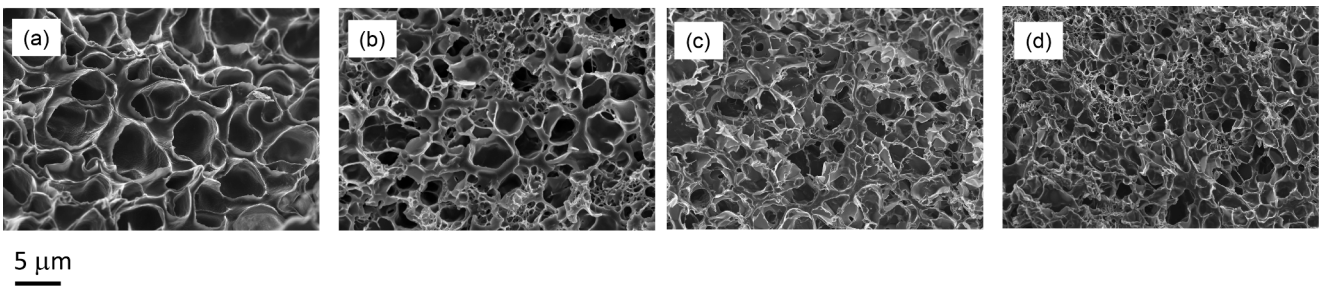

Fig. 6. FE-SEM micrographs: (a) PNIP_F, (b) PNIP_PCL_10_F, (c) PNIP_PCL_20_F and (d) PNIP_PCL_25_F.

such as in poly(-aminoester) (PBAE) crosslinked gels [59] and in semi-IPN structures [60] where the pore size was directly correlated with the degree of crosslinking and the material stiffness. In addition, it is relevant to underline that no PCL aggregates are visible, indicating a fine dispersion of the polyesters in the PNIPAAm phase and supporting the results of the DSC measurements.

3.6. Mechanical characterization of hydrogels

In the present work, the elastic modulus was characterized by two different techniques, namely static and dynamic mechanical analysis. Both types of measurements were performed to validate the developed hydrogels for different applications. In particular, dynamic characterization is important with respect to tissue engineering applications, since biological tissue is subjected to mechecanical stimuli.

The compressive modulus of the neat PNIPAAm hydrogel was compared with that of the PCL-based samples to evidence the influence of the star-shaped polymer on the mechanical behaviour of the developed materials (Fig. 7). In particular, the force–deformation curves of the prepared samples, shown in Fig. 7a, indicate that all the prepared systems exhibited an hyperelastic behavior, typical of hydrogel materials [61,62]. As for the compressive modulus (E_0), PNIP_F showed an E_0 of ca. 100 kPa, a value in agreement with those previously reported in the literature for PNIPAAm hydrogels [8] (Fig. 7b). The presence of PCL led to a relevant increase of E_0, which increased with increasing the star-shaped polymer content in the hydrogels. In particular, it is relevant to underline that in the sample with the highest concentration of PCL-COOH, *i.e.*, PNIP_PCL_25, E_0 was four times higher than in the neat PNIPAAm hydrogel.

This behavior was also confirmed by the results of the DMA used to measure the stiffness of the hydrogel in terms of elastic moduli (E_{20}) as a function of the frequency of the applied compressive load, with a pre-strain of 20% (Fig. S2). Specifically, neat PNIP_F showed an elastic modulus of about 37 kPa, while the samples based on PCL-COOH (10, 20, and 25 wt%), exhibited a drastic and linear increase in elastic moduli: 137.54 ± 23.07 kPa, 185.88 ± 30.59 kPa and 213.57 ± 16.76 kPa, respectively. Overall, the results indicated that the presence of the star shaped polymer contributes to the improvement of mechanical strenght of the PNIPAAm hydrogels. Although, as previously mentioned, it is difficult to make a comparison with data reported in the literature, since the mechanical properties of PNIPAAm-based hydrogels are highly dependent on a number of parameters, the moduli found make the developed material suitable for tissue engineering applications [4].

3.7. Cell viability evaluation

To determine the cytoxicity of the hydrogels on SH-SY5Y cultures, cells were exposed for 48 h to the two extreme conditions: sample without PCL (PNIP_F) and samples with the maximum amount of PCL (PNIP_PCL_25_F). First, SH-SY5Y cells were observed by optical microscopy before the exposition to the different samples (Fig. 8a) and after each 24 h to 48 h. Qualitatively, no differences were observed in both conditions during the time in culture. The live/dead assay showed that PNIP_PCL_25_F did not induce any toxic effect on the cultures of human neuroblastoma cells SH -SY5Y (Fig. 8b). This qualitative observation was confirmed by cell viability quantification shown in Fig. 8c, which was measured by normalizing the number of live cells with the total cell number. Under both conditions, comparable and high viability indexes were observed after 48 h. In particular, cell viability of SH-SY5Y exposed to PNIP_PCL_25_F samples showed a slightly decrease, but the result was not statistically different from that the control.

3.8. Dye absorption and release tests

To evaluate the effect of the addition of PCL-COOH to PNIPAAM on the retention capacity of the system, the prepared xerogels were contacted with a pararosaniline (PR) solution, a cationic dye. The results reported in the in Fig. 9 show the amount of PR absorbed by the hydrogels in their swollen state at 22 °C after 24 h. From the histogram, it can be seen that the amount of PR, retained by PNIP_F was negligible and difficult to estimate precisely due to the very small concentration differences of PR in solution. On the other hand, the quantity of PR

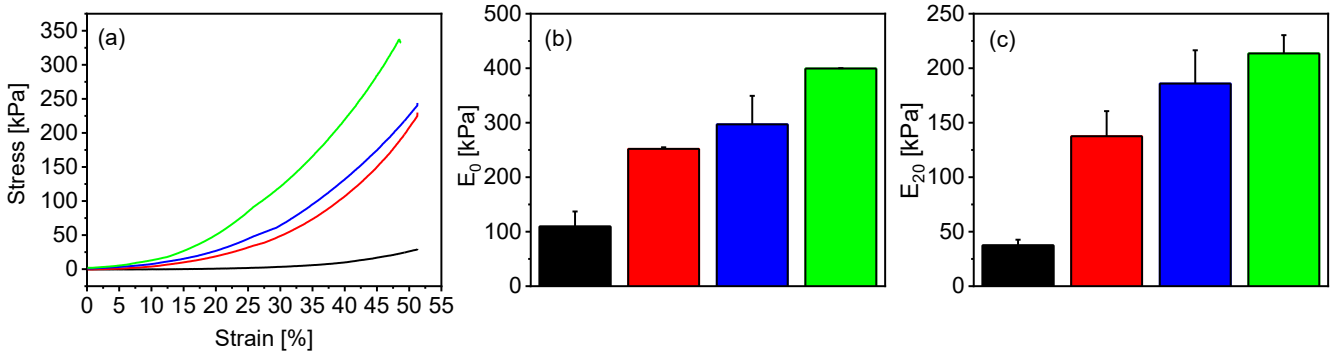

Fig. 7. (a) Force-deformation curve, (b) compressive modulus of PNIP samples from compressive static test, (c) elastic moduli of PNIP samples with and without PCL from DMA.

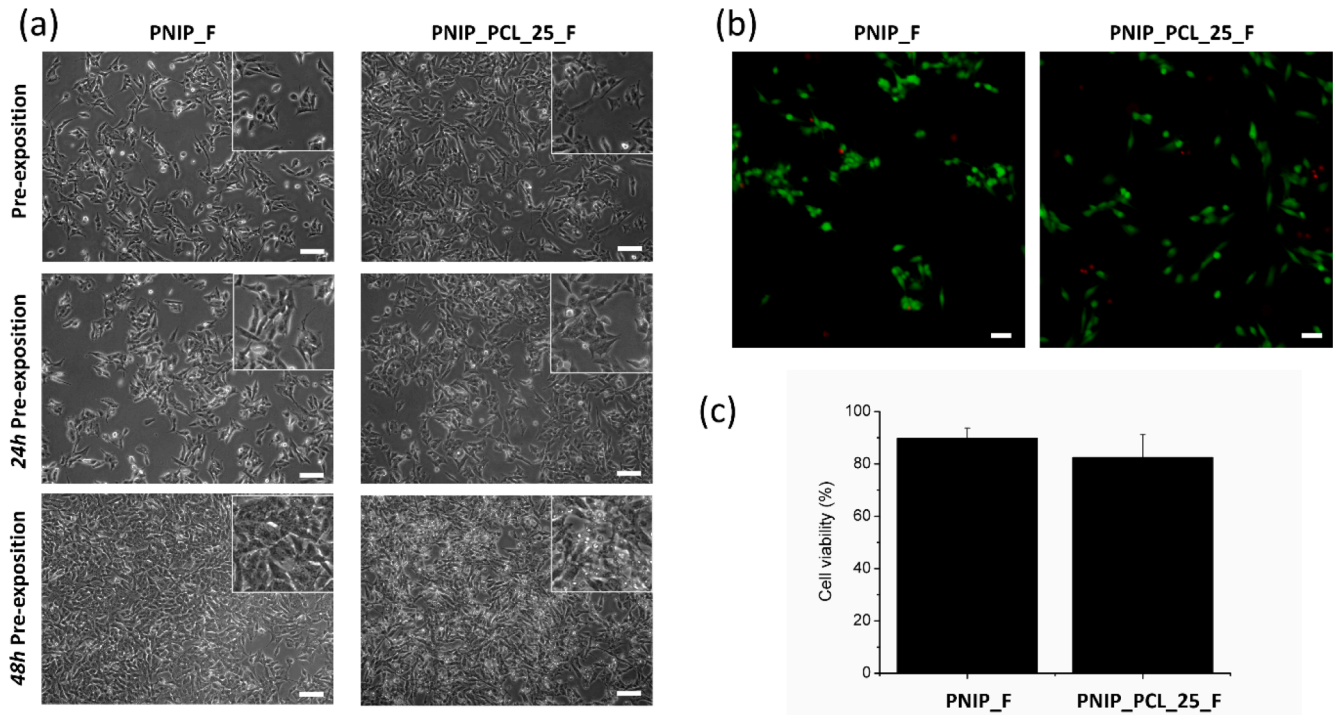

Fig. 8. Cell viability evaluation by (a) Optical contrast phase images of 2D SH-SY5Y cell culture before and 24–48 h after the exposition to PNIP_F an PNIP_PCL_25_F. Scale bars are 50 μm. (b) Live/dead staining with Calcein-AM (green) and EthD-1 (red); scale bars are 50 μm. (c) Percentage of cell viability, defined as the number of live cells divided by the total cell number. (For interpretation of the references to colour in this figure legend, the reader is referred to the web version of this article.)

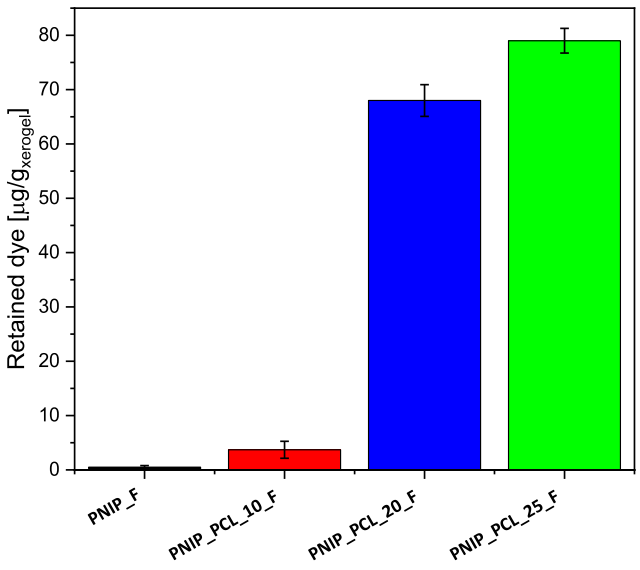

Fig. 9. PR retention at equilibrium at 22 °C, for PNIP_F (black), PNIP_PCL_10_F (red), PNIP_PCL_20_F (blue), PNIP_PCL_25_F (green). (For interpretation of the references to colour in this figure legend, the reader is referred to the web version of this article.)

absorbed by the materials increased steeply with PCL-COOH content and was mainly attributed to the presence of ionized carboxylic moieties, which are capable of interacting with the ionized amino group of PR through non-specific ionic interactions. In this regard, it is worth underling that as the pH of the solution used was 5.4 and the pK_a of PR and maleic end groups in PCL-COOH were 8.8 [63] and 1.9 [64], respectively, it can be concluded that both the amino groups of PR and the carboxy groups of PCL-COOH were present in their ionized form.

Indeed, as previously reported, the presence of the above ionized carboxyl groups ($–COO^-$) is essential for the adsorption of cationic species, such as drugs [65] or pollutants [6&] through the above-mentioned interactions. For example, Yang et al. prepared NIPAAM/acrylic acid/MoS_2 composite copolymer hydrogels by photopolymerization that were able to absorb methylene blue, potentially applicable in wastewater treatment [67]. Similarly, Mahida et al. developed nanohydrogels, by emulsion copolymerization of NIPAAM in combination with acrylic acid and N-allylisatin, capable of adsorbing hazardous cationic dyes [66]. The above works demonstrate the applicability of PNIPAAm-based systems as adsorbents and the need to combine the polymer matrix with suitable materials to make it functional. As for the specific adsorption capacity, the variability of the values found in the literature can be related to both the nature of the substances to be adsorbed as well as to the properties of the adsorbents in terms of concentration of functionalities, porosity, crystallinity, etc.

Dye release was studied by loading the hydrogels with PR and following the amount released over time (Fig. S3). It is worth underling that the lack of controlled release of neat PNIPAAm hydrogels is a significant aspect that could limit their potential application as drug carriers [68].

From the trend of Fig. S2, it can be seen that the release kinetics of the hydrogels were strongly influenced by the sample composition, with curves characterized by an initial burst phase followed by a decrease in the release rate until an equilibrium plateau was reached. In particular, as showed in Fig. S4, the release in the first phase followed a first-order kinetic with an initial release rate (RR_i), reported in Table S4, that was inversely proportional to the PCL amount. Indeed, the introduction of PCL-COOH affected the time required to reach the plateau concentration C_{max}, which increased from 9 h, measured for PNIP_F and PNIP_PCL_10_F, to ca. 30 h, for PNIP_PCL_20_F and PNIP_PCL_25_F samples. Considering the behavior of our PCL-based hydrogels, this may be related to several aspects, such as the specific interactions which occur between the PCL functionalities and the dye as well as the physical properties of the hydrogel, which are modified by the presence of the star-shaped polymer. Regarding the latter feature, the diffusion of the

dye in the hydrogels could also be reduced by the crystallinity imparted to the system by the presence of PCL-COOH and by the lower porosity of the PCL-based systems compared that of the neat PNIPAAm hydrogels.

4. Conclusions

In this work, novel PNIPAAm-based hydrogels were developed with high mechanical strength, ability to interact with positively charged molecules with tunable kinetic release and swelling ratio, biocompatibility, and thermoresponsiveness. Indeed, the above properties were achieved by adding to the reaction mixture a star-shaped PCL, synthesized *ad-hoc* using an environmentally friendly method, ending with maleic groups (PCL-COOH) that enable the polymer to participate in the polymerization process and impart active functionalities. In addition, the effectiveness of the frontal polymerization in the development of PNIPAAm/PCL-COOH hydrogels was demonstrated, which is a fast and efficient polymerization method, capable to guarantee a fine dispersion of the star-shaped polymer in the PNIPAAm matrix.

CRediT authorship contribution statement

Giacomo Damonte: Investigation, Visualization, Writing – original draft. **Martina Cozzani:** Investigation, Visualization. **Donatella Di Lisa:** Investigation, Visualization. **Laura Pastorino:** Investigation, Visualization. **Alberto Mariani:** Conceptualization, Writing – review & editing. **Orietta Monticelli:** Conceptualization, Supervision, Writing – review & editing.

Declaration of Competing Interest

The authors declare that they have no known competing financial interests or personal relationships that could have appeared to influence the work reported in this paper.

Data availability

Data will be made available on request.

Appendix A. Supplementary data

Supplementary data to this article can be found online at https://doi.org/10.1016/j.eurpolymj.2023.112239.

References

[1] S. Ziane, S. Schlaubitz, S. Miraux, A. Patwa, C. Lalande, I. Bilem, S. Lepreux, B. Rousseau, J.-F. Le Meins, L. Latxague, O.C. Barthélémy, A thermosensitive low molecular weight hydrogel as scaffold for tissue engineering, Eur. Cells Mater. 23 (2012) 147–160. https://doi.org/10.22203/eCM.v023a11.

[2] Y. Zhao, C. Shi, X. Yang, B. Shen, Y. Sun, Y. Chen, X. Xu, H. Sun, K. Yu, B. Yang, Q. Lin, pH- and Temperature-Sensitive hydrogel nanoparticles with dual photoluminescence for bioprobes, ACS Nano. 10 (2016) 5856–5863, https://doi.org/10.1021/acsnano.6b00770.

[3] L. Nie, J. Li, G. Lu, X. Wei, Y. Deng, S. Liu, S. Zhong, Q. Shi, R. Hou, Y. Sun, C. Politis, L. Fan, O.V. Okoro, A. Shavandi, Temperature responsive hydrogel for cells encapsulation based on graphene oxide reinforced poly(N-isopropylacrylamide)/hydroxyethyl-chitosan, Mater. Today Commun. 31 (2022), 103697, https://doi.org/10.1016/j.mtcomm.2022.103697.

[4] M.A. Haq, Y. Su, D. Wang, Mechanical properties of pnipam based hydrogels: a review, Mater. Sci. Eng. C. 70 (2017) 842–855, https://doi.org/10.1016/j.msec.2016.09.081.

[5] E. Ho, A. Lowman, M. Marcolongo, Synthesis and characterization of an injectable hydrogel with tunable mechanical properties for soft tissue repair, Biomacromolecules 7 (2006) 3223–3228, https://doi.org/10.1021/bm0602536.

[6] S. Petrusic, M. Lewandowski, S. Giraud, P. Jovancic, B. Bugarski, S. Ostojic, V. Koncar, Development and characterization of thermosensitive hydrogels based on poly(N-isopropylacrylamide) and calcium alginate, J. Appl. Polym. Sci. 124 (2012) 890–903, https://doi.org/10.1002/app.35122.

[7] R. Fei, J.T. George, J. Park, M.A. Grunlan, Thermoresponsive nanocomposite double network hydrogels, Soft Matter. 8 (2012) 481–487, https://doi.org/10.1039/C1SM06105D.

[8] R. Fei, J.T. George, J. Park, A.K. Means, M.A. Grunlan, Ultra-strong thermoresponsive double network hydrogels, Soft Matter. 9 (2013) 2912, https://doi.org/10.1039/c3sm27226e.

[9] Z. Li, J. Shen, H. Ma, X. Lu, M. Shi, N. Li, M. Ye, Preparation and characterization of ph- and temperature-responsive nanocomposite double network hydrogels, Mater. Sci. Eng. C. 33 (2013) 1951–1957, https://doi.org/10.1016/j.msec.2013.01.004.

[10] X. Ma, Y. Li, W. Wang, Q. Ji, Y. Xia, Temperature-sensitive poly(N-isopropylacrylamide)/graphene oxide nanocomposite hydrogels by in situ polymerization with improved swelling capability and mechanical behavior, Eur. Polym. J. 49 (2013) 389–396, https://doi.org/10.1016/j.eurpolymj.2012.10.034.

[11] K. Van Durme, B. Van Mele, W. Loos, F.E. Du Prez, Introduction of silica into thermo-responsive poly(N-isopropyl acrylamide) hydrogels: a novel approach to improve response rates, Polymer 46 (2005) 9851–9862, https://doi.org/10.1016/j.polymer.2005.08.032.

[12] B. Strachotová, A. Strachota, M. Uchman, M. Šlouf, J. Brus, J. Pleštil, L. Matějka, Super porous organic–inorganic poly(N-isopropylacrylamide)-based hydrogel with a very fast temperature response, Polymer 48 (2007) 1471–1482, https://doi.org/10.1016/j.polymer.2007.01.042.

[13] S.B. Campbell, M. Patenaude, T. Hoare, Injectable superparamagnets: highly elastic and degradable Poly(N-isopropylacrylamide)–superparamagnetic iron oxide nanoparticle (spion) composite hydrogels, Biomacromolecules 14 (2013) 644–653, https://doi.org/10.1021/bm301703x.

[14] G. Marcelo, M. López-González, F. Mendicuti, M.P. Tarazona, M. Valiente, Poly(N-isopropylacrylamide)/gold hybrid hydrogels prepared by catechol redox chemistry. characterization and smart tunable catalytic activity, Macromolecules 47 (2014) 6028–6036, https://doi.org/10.1021/ma501214k.

[15] G. Huerta-Angeles, K. Hishchak, A. Strachota, B. Strachota, M. Šlouf, L. Matějka, Super-porous nanocomposite pnipam hydrogels reinforced with titania nanoparticles, displaying a very fast temperature response as well as ph-sensitivity, Eur. Polym. J. 59 (2014) 341–352, https://doi.org/10.1016/j.eurpolymj.2014.07.033.

[16] Q. Zhang, T. Zhang, T. He, L. Chen, Removal of crystal violet by clay/pnipam nanocomposite hydrogels with various clay contents, Appl. Clay Sci. 90 (2014) 1–5, https://doi.org/10.1016/j.clay.2014.01.003.

[17] T. Huang, P(nipam-co-aa)/clay nanocomposite hydrogels exhibiting high swelling ratio accompanied by excellent mechanical strength, Appl. Phys. A Mater. Sci. Process. 107 (2012) 905–909, https://doi.org/10.1007/s00339-012-6817-6.

[18] K. Haraguchi, R. Farnworth, A. Ohbayashi, T. Takehisa, Compositional effects on mechanical properties of nanocomposite hydrogels composed of poly(N, N-dimethylacrylamide) and clay, Macromolecules 36 (2003) 5732–5741, https://doi.org/10.1021/ma034366i.

[19] W.-F. Lee, T.-S. Cheng, Studies on preparation and properties of porous biodegradable poly(nipaam) hydrogels, J. Appl. Polym. Sci. 109 (2008) 1982–1992, https://doi.org/10.1002/app.28370.

[20] R. París, I. Quijada-Garrido, Swelling and hydrolytic degradation behaviour of ph-responsive hydrogels of poly[(N-isopropylacrylamide)-co-(methacrylic acid)] crosslinked by biodegradable polycaprolactone chains, Polym. Int. 58 (2009) 362–367, https://doi.org/10.1002/pi.2539.

[21] G.T. Chao, Z.Y. Qian, M.J. Huang, B. Kan, Y.C. Gu, C.Y. Gong, J.L. Yang, K. Wang, M. Dai, X.Y. Li, M.L. Gou, M.J. Tu, Y.Q. Wei, Synthesis, characterization, and hydrolytic degradation behavior of a novel biodegradable pH-sensitive hydrogel based on polycaprolactone, methacrylic acid, and poly(ethylene glycol), J. Biomed. Mater. Res. Part A 85A (2008) 36–46, https://doi.org/10.1002/jbm.a.31362.

[22] B.A. Suslick, J. Hemmer, B.R. Groce, K.J. Stawiasz, P.H. Geubelle, G. Malucelli, A. Mariani, J.S. Moore, J.A. Pojman, N.R. Sottos, Frontal polymerizations: from chemical perspectives to macroscopic properties and applications, Chem. Rev. 123 (2023) 3237–3298, https://doi.org/10.1021/acs.chemrev.2c00686.

[23] G. Damonte, B. Barsanti, A. Pellis, G.M. Guebitz, O. Monticelli, On the effective application of star-shaped polycaprolactones with different end functionalities to improve the properties of polylactic acid blend films, Eur. Polym. J. 176 (2022), 111402, https://doi.org/10.1016/j.eurpolymj.2022.111402.

[24] G. Damonte, A. Vallin, D. Battegazzore, A. Fina, O. Monticelli, Synthesis and characterization of a novel star polycaprolactone to be applied in the development of graphite nanoplates-based nanopapers, React. Funct. Polym. 167 (2021), 105019, https://doi.org/10.1016/j.reactfunctpolym.2021.105019.

[25] G. Damonte, F. Cantamessa, A. Fina, O. Monticelli, Star-shaped furoate-pcl: an effective compound for the development of graphite nanoplatelets-based films, React. Funct. Polym. 184 (2023), 105515, https://doi.org/10.1016/j.reactfunctpolym.2023.105515.

[26] E.R. Leone, L.S. Ferraraccio, G. Damonte, P. Lova, P. Bertoncello, O. Monticelli, On the development of electrochemical sensors coated with polycaprolactone, Electrochem. Commun. 129 (2021), 107089, https://doi.org/10.1016/j.elecom.2021.107089.

[27] J. Masere, Y. Chekanov, J.R. Warren, F.D. Stewart, R. Al-Kaysi, J.K. Rasmussen, J. A. Pojman, Gas-free initiators for high-temperature free-radical polymerization, J. Polym. Sci. Part A Polym. Chem. 38 (2000) 3984–3990, https://doi.org/10.1002/1099-0518(20001101)38:21<3984::AID-POLA160>3.0.CO;2-Z.

[28] A. Mariani, D. Nuvoli, V. Alzari, M. Pini, Phosphonium-based ionic liquids as a new class of radical initiators and their use in gas-free frontal polymerization, Macromolecules 41 (2008) 5191–5196, https://doi.org/10.1021/ma800610g.

[29] M.A. Woodruff, D.W. Hutmacher, The return of a forgotten polymer - polycaprolactone in the 21st century, Prog. Polym. Sci. 35 (2010) 1217–1256, https://doi.org/10.1016/j.progpolymsci.2010.04.002.

[30] J.A. Pojman, G. Curtis, V.M. Ilyashenko, Frontal polymerization in solution, J. Am. Chem. Soc. 118 (1996) 3783–3784, https://doi.org/10.1021/ja9600688.

[31] N. do Nascimento Marques, P.S. Curti, A.M. da Silva Maia, R.d.C. Balaban, Temperature and ph effects on the stability and rheological behavior of the aqueous suspensions of smart polymers based on N-isopropylacrylamide, chitosan, and acrylic acid, J. Appl. Polym. Sci. 129 (1) (2013) 334–345.
[32] C. Erbil, Y. Yıldız, N. Uyanık, Effects of synthesis-solvent composition and initiator concentration on the swelling behaviour of poly(N-isopropylacrylamide) p (nipaam), poly(nipaam-co-dimethyl itaconate), and poly(nipaam-co-itaconic acid) gels, Polym. Int. 49 (2000) 795–800, https://doi.org/10.1002/1097-0126(200007)49:7<795::AID-PI457>3.0.CO;2-9.
[33] W. Liu, B. Zhang, W.W. Lu, X. Li, D. Zhu, K. De Yao, Q. Wang, C. Zhao, C. Wang, A rapid temperature-responsive sol-gel reversible poly(N-isopropylacrylamide)-g-methylcellulose copolymer hydrogel, Biomaterials 25 (2004) 3005–3012, https://doi.org/10.1016/j.biomaterials.2003.09.077.
[34] X. Hu, Z. Tong, L.A. Lyon, Control of poly(N-isopropylacrylamide) microgel network structure by precipitation polymerization near the lower critical solution temperature, Langmuir 27 (2011) 4142–4148, https://doi.org/10.1021/la200114s.
[35] N. Milašinović, Z. Knežević-Jugović, N. Milosavljević, M. Lučić Škorić, J. Filipović, M., Kalagasidis Krušić, Stimuli-sensitive hydrogel based on n-isopropylacrylamide and itaconic acid for entrapment and controlled release of candida rugosa lipase under mild conditions, Biomed Res. Int. (2014 (2014)) 1–9, https://doi.org/10.1155/2014/364930.
[36] A. Vallin, D. Battegazzore, G. Damonte, A. Fina, O. Monticelli, On the development of nanocomposite covalent associative networks based on polycaprolactone and reduced graphite oxide, Nanomaterials 12 (2022) 3744, https://doi.org/10.3390/nano12213744.
[37] M. Biswas, J.A. Libera, S.B. Darling, J.W. Elam, Polycaprolactone: a promising addition to the sequential infiltration synthesis polymer family identified through in situ infrared spectroscopy, ACS Appl. Polym. Mater. 2 (2020) 5501–5510, https://doi.org/10.1021/acsapm.0c00855.
[38] R.G. Sousa, W.F. Magalhães, R.F.S. Freitas, Glass transition and thermal stability of poly(N-isopropylacrylamide) gels and some of their copolymers with acrylamide, Polym. Degrad. Stab. 61 (1998) 275–281, https://doi.org/10.1016/S0141-3910(97)00209-7.
[39] G. Damonte, L. Maddalena, A. Fina, D. Cavallo, A.J. Müller, M.R. Caputo, A. Mariani, O. Monticelli, On novel hydrogels based on poly(2-hydroxyethyl acrylate) and polycaprolactone with improved mechanical properties prepared by frontal polymerization, Eur. Polym. J. 171 (2022), 111226, https://doi.org/10.1016/j.eurpolymj.2022.111226.
[40] L. Sangroniz, B. Wang, Y. Su, G. Liu, D. Cavallo, D. Wang, A.J. Müller, Fractionated crystallization in semicrystalline polymers, Prog. Polym. Sci. 115 (2021), 101376, https://doi.org/10.1016/j.progpolymsci.2021.101376.
[41] S. Nojima, M. Toei, S. Hara, S. Tanimoto, S. Sasaki, Size dependence of crystallization within spherical microdomain structures, Polymer 43 (2002) 4087–4090, https://doi.org/10.1016/S0032-3861(02)00217-3.
[42] A.J. Müller, V. Balsamo, M.L. Arnal, T. Jakob, H. Schmalz, V. Abetz, Homogeneous nucleation and fractionated crystallization in block copolymers, Macromolecules 35 (2002) 3048–3058, https://doi.org/10.1021/ma012026w.
[43] A.J. Müller, V. Balsamo, M.L. Arnal, in: Nucleation and Crystallization in Diblock and Triblock Copolymers, Springer-Verlag, Berlin/Heidelberg, 2005, pp. 1–63, https://doi.org/10.1007/12_001.
[44] R.V. Castillo, A.J. Müller, J.-M. Raquez, P. Dubois, Crystallization kinetics and morphology of biodegradable double crystalline plla-b-pcl diblock copolymers, Macromolecules 43 (2010) 4149–4160, https://doi.org/10.1021/ma100201g.
[45] L. Tavagnacco, E. Zaccarelli, E. Chiessi, On the molecular origin of the cooperative coil-to-globule transition of poly(N-isopropylacrylamide) in water, Phys. Chem. Chem. Phys. 20 (2018) 9997–10010, https://doi.org/10.1039/C8CP00537K.
[46] M. Zhang, Y. Li, Q. Yang, L. Huang, L. Chen, H. Xiao, Adsorption of methyl violet using pH- and temperature-sensitive cellulose filament/poly(nipam-co-aac) hybrid hydrogels, J. Mater. Sci. 53 (2018) 11837–11854, https://doi.org/10.1007/s10853-018-2342-0.
[47] A. Sosnik, J.C. Imperiale, B. Vázquez-González, M.M. Raskin, F. Muñoz-Muñoz, G. Burillo, G. Cedillo, E. Bucio, Mucoadhesive thermo-responsive chitosan-g-poly (N-isopropylacrylamide) polymeric micelles via a one-pot gamma-radiation-assisted pathway, Colloids Surfaces B Biointerfaces 136 (2015) 900–907, https://doi.org/10.1016/j.colsurfb.2015.10.036.
[48] A.S. Patil, A.P. Gadad, R.D. Hiremath, P.M. Dandagi, Exploration of the effect of chitosan and crosslinking agent concentration on the properties of dual responsive chitosan-g-poly(N-isopropylacrylamide) co-polymeric Particles, J. Polym. Environ. 26 (2018) 596–606, https://doi.org/10.1007/s10924-017-0971-z.
[49] H.G. Schild, Thermal decomposition of pnipaam: tga-ftir analysis, J. Polym. Sci. Part A Polym. Chem. 34 (1996) 2259–2262, https://doi.org/10.1002/(SICI)1099-0518(199608)34:11<2259::AID-POLA21>3.0.CO;2-D.
[50] M. Unger, C. Vogel, H.W. Siesler, Molecular weight dependence of the thermal degradation of poly(ε-caprolactone): a thermogravimetric differential thermal fourier transform infrared spectroscopy study, Appl. Spectrosc. 64 (2010) 805–809, https://doi.org/10.1366/000370210791666309.
[51] S. Li, X. Liu, Synthesis, characterization, and evaluation of enzymatically degradable poly(N-isopropylacrylamide-co-acrylic acid) hydrogels for colon-specific drug delivery, Polym. Adv. Technol. 19 (2008) 1536–1542, https://doi.org/10.1002/pat.1162.
[52] C.S. Biswas, V.K. Patel, N.K. Vishwakarma, A.K. Mishra, R. Bhimireddi, R. Rai, B. Ray, Synthesis, characterization, and drug release properties of poly(N-isopropylacrylamide) gels prepared in methanol-water cononsolvent medium, J. Appl. Polym. Sci. 125 (2012) 2000–2009, https://doi.org/10.1002/app.36318.
[53] C. Yu, Z. Duan, P. Yuan, Y. Li, Y. Su, X. Zhang, Y. Pan, L.L. Dai, R.G. Nuzzo, Y. Huang, H. Jiang, J.A. Rogers, Electronically programmable, reversible shape change in two- and three-dimensional hydrogel structures, Adv. Mater. 25 (2013) 1541–1546, https://doi.org/10.1002/adma.201204180.
[54] I. Bischofberger, V. Trappe, New aspects in the phase behaviour of poly-N-isopropyl acrylamide: systematic temperature dependent shrinking of pnipam assemblies well beyond the LCST, Sci. Rep. 5 (2015) 15520, https://doi.org/10.1038/srep15520.
[55] S.J. Lue, C.-H. Chen, C.-M. Shih, Tuning of lower critical solution temperature (lcst) of poly(N-isopropylacrylamide-co-acrylic acid) hydrogels, J. Macromol. Sci. Part B. 50 (2011) 563–579, https://doi.org/10.1080/00222341003784550.
[56] M. Kubo, M. Higuchi, T. Koshimura, E. Shoji, T. Tsukada, Control of the temperature responsiveness of poly(N-isopropylacrylamide-co-2-hydroxyethyl methacrylate) copolymer using ultrasonic irradiation, Ultrason. Sonochem. 79 (2021), 105752, https://doi.org/10.1016/j.ultsonch.2021.105752.
[57] K. Son, J. Lee, Synthesis and characterization of poly(ethylene glycol) based thermo-responsive hydrogels for cell sheet engineering, Materials 9 (2016) 854, https://doi.org/10.3390/ma9100854.
[58] J. Su, Y. Yang, Z. Chen, J. Zhou, X. Liu, Y. Fang, Y. Cui, Preparation and performance of thermosensitive poly(N-isopropylacrylamide) hydrogels by frontal photopolymerization, Polym. Int. 68 (2019) 1673–1680, https://doi.org/10.1002/pi.5868.
[59] Y. Balçık Tamer, A new design of poly(N-isopropylacrylamide) hydrogels using biodegradable poly(beta-aminoester) crosslinkers as fertilizer reservoirs for agricultural applications, Gels 9 (2023) 127. https://doi.org/10.3390/gels9020127.
[60] S.-P. Rwei, H. Tuan, W.-Y. Chiang, T.-F. Way, Synthesis and characterization of ph and thermo dual-responsive hydrogels with a semi-ipn structure based on n-isopropylacrylamide and itaconamic acid, Materials 11 (2018) 696, https://doi.org/10.3390/ma11050696.
[61] A. Sasson, S. Patchornik, R. Eliasy, D. Robinson, R. Haj-Ali, Hyperelastic mechanical behavior of chitosan hydrogels for nucleus pulposus replacement - experimental testing and constitutive modeling, J. Mech. Behav. Biomed. Mater. 8 (2012) 143–153, https://doi.org/10.1016/J.JMBBM.2011.12.008.
[62] J. Gan, X.X. Guan, J. Zheng, H. Guo, K. Wu, L. Liang, M. Lu, Biodegradable, thermoresponsive pnipam-based hydrogel scaffolds for the sustained release of levofloxacin, RSC Adv. 6 (2016) 32967–32978, https://doi.org/10.1039/c6ra03045a.
[63] H. Da Silva Junior, G.R.S. De Freitas, D.R.F. Néri, F.R.D.S. Pereira, R.F. De Farias, F.C. Pereira, Monitoramento do corante pararosanilina em amostras biológicas, Eclética Química J. 35 (2018) 147. https://doi.org/10.26850/1678-4618eqj.v35.3.2010.p147-156.
[64] F.R. Trull, S. Boiadjiev, D.A. Lightner, A.F. McDonagh, Aqueous dissociation constants of bile pigments and sparingly soluble carboxylic acids by ^{13}C NMR in aqueous dimethyl sulfoxide: effects of hydrogen bonding, J. Lipid Res. 38 (1997) 1178–1188, https://doi.org/10.1016/S0022-2275(20)37200-X.
[65] R.L. Bartlett, M.R. Medow, A. Panitch, B. Seal, Hemocompatible poly(nipam-mba-amps) colloidal nanoparticles as carriers of anti-inflammatory cell penetrating peptides, Biomacromolecules 13 (4) (2012) 1204–1211.
[66] V.P. Mahida, M.P. Patel, Removal of some most hazardous cationic dyes using novel poly (nipaam/aa/N-allylisatin) nanohydrogel, Arab. J. Chem. 9 (2016) 430–442, https://doi.org/10.1016/j.arabjc.2014.05.016.
[67] J. Yang, K. Wang, Z. Lv, W. Li, K. Luo, Z. Cao, facile preparation and dye adsorption performance of poly(N-isopropylacrylamide-co-acrylic acid)/molybdenum disulfide composite hydrogels, ACS Omega 6 (2021) 28285–28296, https://doi.org/10.1021/acsomega.1c04433.
[68] M.J. Ansari, R.R. Rajendran, S. Mohanto, U. Agarwal, K. Panda, K. Dhotre, R. Manne, A. Deepak, A. Zafar, M. Yasir, S. Pramanik, Poly(N-isopropylacrylamide)-based hydrogels for biomedical applications: a review of the state-of-the-art, Gels 8 (2022) 454, https://doi.org/10.3390/gels8070454.